IJRAME

INTERNATIONAL JOURNAL OF RESEARCH IN AERONAUTICAL AND MECHANICAL ENGINEERING
WWW.IJRAME.COM
ISSN (ONLINE): 2321-3051

Emerging Trends in Mechanical Engineering Proceedings of the International Conference, ETME-2017, 27 & 28 December, 2017, Pg: -102-113

SELECTIVE LOCALIZATION OF CONDUCTING FILLER AND HIGH K MATERIAL IN CO-CONTINUOUS SEMI-CYSTALLINE BLENDS

Dr. Rathnakar.G[1], Swarnakiran.S[2]

[1]*Professor* Dept. of Mech. Engg. ATME College of Engineering. Mysuru.
rathnakar.g.devaru@gmail.com
[2] *Assistant Professor* Dept. of Mech. Engg. ATME College of Engineering. Mysuru.
swarna23raj@gmail.com

Abstract

70/30 blends of polar macromolecules (PVDF/PA6) were prepared by melt-mixing along with MWCNTs, non-covalantly modified MWCNTs and high K material for electromagnetic interference (EMI) shielding applications. The MWCNTs are restricted to only the minority phase due to high wetting factor of melt PA6. Non-covalant modification of MWCNTs with PTCD due to the π- π interaction helps in better network formation leading to enhanced conductivity. Further, a novel approach of adding functionalized ferroelectric material, amine functionalized Barium Titinate, is dispersed in both the matrix along with the conducting filler in the PA6 to help in the absorption of the internally reflected fields. A reflection loss of 53 dB is obtained at 16GHz for the PTCD-MWCNTs and BT-NH_2 nano-composite system.

Introduction:

Poly (Vinylidene fluoride) (PVDF) is a semi crystalline engineering thermoplastic with good thermal, chemical ferroelectric, piezoelectric and pyro electric properties. The abundance of commercial application of electro active polymers make PVDF a popular choice of material in this field. Inherently, PVDF displays excellent thermal and chemical stability[1] along with good mechanical property that has its uses ranging from electrode binders to biomedical applications[2]. PVDF displays multiple crystalline phases like α, β, γ and δ with α and β being the most predominant of the four[3-7]. The α-phase is the most thermodynamically stable of the two. The H and F group within this molecular chain take the most stable conformation with them alternating on both sides. However, the interest lies in the electro active β-polymorph that contain H and F on opposite sides inducing a permanent dipole moment that opens up various piezoelectric

IJRAME

INTERNATIONAL JOURNAL OF RESEARCH IN AERONAUTICAL AND MECHANICAL ENGINEERING
WWW.IJRAME.COM
ISSN (ONLINE): 2321-3051

Emerging Trends in Mechanical Engineering Proceedings of the International Conference, ETME-2017, 27 & 28 December, 2017, Pg: -102-113

applications. Several strategies like application of electric field, thermal annealing, stretching[8], mechanical drawing[9] and polar additives[10] have been employed to induce this electro active phase of PVDF. PVDF cooled from the melt phase predominantly forms the α-phase due to the high crystallization rate and on application of stress at lower temperatures, the molecular chain reorients to form the electro active the β-phase. Poly Amide 6 (PA6) is blended to incept the piezoelectric phase in the PVDF. Due to the high cost of PVDF, this provides a perfect opportunity to bring out the balance between cost and application. There are reports of many classical approach of inducing β-polymorph by blending with polar macromolecules, where the dipoles of the second matrix interact during crystallization that helps orient the PVDF to form the β-polymorph. PA6 in this case is the polar material that is added in minor amount in an attempt to manifest the polar crystal forms of PVDF which exhibits ferroelectric properties due to existence of net dipoles. PA6 is a semi

Conductive fillers such as MWCNTs are often used as a shortcut to induce conductivity into polymers. Polymer blends or alloys can be exploited for added head start to attain the best of both materials decreasing the intricacy of completely modifying a single material and also maintaining its indigenous properties. Majority The ease of producing this conductive nanocomposite is unparalled as it required only the melt mixing of the raw materials. A synergistic effect is expected of the conductive nature of the percolated MWCNTs structure and the formation of piezoelectric phase of the β-polymorph that could possibly be a tailor-made light weight and corrosion free material[11] for EMI shielding applications[12-17].

Addition of high k- material such as Barium Titanate (BaTiO3) is a cost effective ferroelectric material popularly used in the field of EMI shielding at high frequencies[15]. The high dielectric constant at high frequency is attributed to the domain body inertia. $BaTiO_3$. The effectiveness of the high dielectric constant and permittivity are dependent on the grain size and internal connectivity[18]. Ceramics added at high percentage into the matrix percolate to form an interconnecting network structure. Although BaTiO3 has a dielectric constant of above 1000, the material displays low effective dielectric constant when included into the matrix. This is mainly due to the poor internal connectivity and the dielectric constant is majorly dependent on the matrix system the high-k material used[15]. Polymers are inherently low dielectric constant materials and hence the need of the β-polymorph PVDF. Muralidhar et al.[19] studied about the dielectric properties of the PVDF-$BaTiO_3$ composite based on morphology and discusses about the dielectric, resistivity and hysteresis behavior of the composite.

In this study, PVDF and PA6 were used as the polymer matrix blend. This particular blend being influenced by the fact that PVDF shows piezoelectric β-polymorphs in the presence of a polar matrix nylon 6 and with the inclusion of nano-particles. Various strategies were adopted using MWCNTs or nano-particles to facilitate the electro active β-polymorph in PVDF for the 70-30 PVDF-PA6 blend system. Further, the effect of non-covalently modified MWCNTs along with modified high K materials (Barium Titanate) has been systematically evaluated with respect to the

IJRAME

INTERNATIONAL JOURNAL OF RESEARCH IN AERONAUTICAL AND MECHANICAL ENGINEERING
WWW.IJRAME.COM
ISSN (ONLINE): 2321-3051

Emerging Trends in Mechanical Engineering Proceedings of the International Conference, ETME-2017, 27 & 28 December, 2017, Pg: -102-113

fraction of electro active β-polymorph developed in PVDF. FTIR study was conducted to characterize the structure developed under the various nano-particle system. The room temperature AC electrical conductivity was calculated to observe the dispersion and percolation of the MWCNTs added to the blend system. This analysis could be further used to confirm the co-continuous nature of PA6 in the system. Further, an attempt was made to correlate the changes observed in the crystal structure and percolated network formation of the conducting nano-particle with the electric and EMI shielding properties.

Experimental Section:

Materials:

PVDF has been procured from Arkema Inc. (Kynar-761) with molecular weight of 440 000 g mol^{-1}. PA6 1022B were generously provided by Ube industries. The pristine MWCNTs, with average diameter 9.5 nm and average length 1.5 µm were obtained from Nanocyl SA (Belgium). The purity of the MWCNT used was close to 90%. The average particle size of Barium Titanate (BT) obtained from Sigma Aldrich was 100nm. 3,4,9,10-perylenetetracarboxylic dianhydride (PTCD), 4,4′methylenedianiline (MDA) and 3-aminopropyltriethoxysilane (APTS) were obtained from Sigma Aldrich.

Preparation of PTCD MWCNTs:

PTCD and MWCNTs of 100 mg each is dispersed together in 100 ml of DMF. The mixture was bath sonicated for 2 h for complete penetration of PTCD and homogenous dispersion of MWCNTs. The mixture was then vigorously stirred using a magnetic stirrer at room temperature for 12 h. The homogenous mixture is then kept overnight for aging. Post aging, the mixture was filtered and then dried under vacuum at 80 ^{0} C for 24 h.

Preparation of 3-aminopropyltriethoxysilane (APTS) coated BT nanoparticles:

The preparation of NH2 functionalized BT nanoparticles is a two-step process. First, the BT was mixed in H_2O_2 and was then bath sonicated for 30 min. The resulting well dispersed mixture was refluxed at 105 ^{0} C for 4 h and then dried at 100 ^{0} C under vacuum. In the second step, hydroxyl groups induced on BT is reacted with ATPS followed by reflux at 80 ^{0} C under inert atmosphere for 24 h. The unreacted APTS was then centrifuges and washed with toluene. This step was repeated until all of the unreacted APTS was removed. It was then dried under vacuum at 80 ^{0} C for 24 h. The final yield obtained was NH_2 terminated BT.

IJRAME

INTERNATIONAL JOURNAL OF RESEARCH IN AERONAUTICAL AND MECHANICAL ENGINEERING
WWW.IJRAME.COM
ISSN (ONLINE): 2321-3051

Emerging Trends in Mechanical Engineering Proceedings of the International Conference, ETME-2017, 27 & 28 December, 2017, Pg: -102-113

Blend Preparation:

70/30 (wt./wt.) PVDF/PA6 neat blends were prepared by melt-mixing using the mini II HAAKE extruder (7 cm^3) at 250 ^{0} C. The screw speed was maintained constantly at 60 rpm for 20 min. All blends were prepared in inert atmosphere to prevent oxidization. The immiscible blend system was expected to have co-continuous morphology. Further composite batches with 70/30 matrix composition were prepared with the addition of 3 wt. % of pristine CNTs. Generally, pristine MWCNTs agglomerate due to its high aspect ratio, specific surface area and π-π interaction. In order for efficient dispersion and conductivity, it is necessary to pre-process the MWCNTs. 100 mg of MWCNTs and 100ml of THF was taken into a 250ml beaker. This mixture was probe sonicated for 15 min to de-bundle the agglomerated MWCNTs. This mixture was then bath sonicated for 45 min to disperse the MWCNTs completely. The MWCNTs was then vigorously stirred until the THF was mostly removed. The MWCNTs were table dried and then placed in the oven at 80 ^{0} C under vacuum for 24 h. This processed MWCNTs (p-MWCNTs) was added to the blend and melt mixed maintaining the above conditions. Similar procedures were followed to prepare the other batches with 3 wt. % PTCD-MWCNTs and 3 wt. % PTCD-MWCNTs along with 5% vol. amine terminated BT. The melt mixed samples were then molded at 250 ^{0} C using a lab scale hydraulic press to prepare specimens for different tests. All the raw materials were dried at 80 ^{0} C in vacuum for 24 h before processing.

Characterization:

The Fourier transform infrared (FT-IR) spectroscopy analysis was carried out using PerkinElmer GX in the range of 4000-650 cm^{-1}. Morphological analyses for various blends were assessed using an ULTRA 55 scanning electron microscope (SEM).
The thermal properties of neat PVDF and various blends were studied using TA instruments Q2000 differential scanning calorimeter (DSC) in temperature range of -50 ^{0} C to 220 ^{0} C.
The AC electrical conductivity for nanocomposites was analyzed in frequency range of 0.1 Hz to 10 MHz using Alpha-N Analyzer, Novocontrol (Germany). The room temperature AC conductivity was measured on 1mm thick compression molded disks.
The EMI shielding experiment were carried out using vector network analyzer (VNA), Anritsu MS4642A in X and K_u-band frequency range. The coax set up (Damaskos M07T) connected to VNA was used as sample holder for compression molded toroidal specimen. The sample holder and transmission lines were calibrated using complete two ports SOLT (short-open-load-transmission) method. The various scattering parameters were extracted in X and K_u-band frequency range.

IJRAME

INTERNATIONAL JOURNAL OF RESEARCH IN AERONAUTICAL AND MECHANICAL ENGINEERING
WWW.IJRAME.COM
ISSN (ONLINE): 2321-3051

Emerging Trends in Mechanical Engineering Proceedings of the International Conference, ETME-2017, 27 & 28 December, 2017, Pg: -102-113

Results and discussion:

β -*phase formation:*

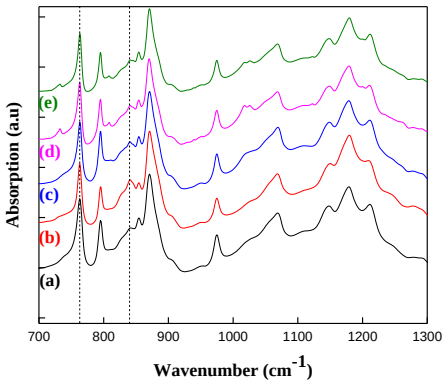

Figure 1: FT-Ir Plot of (a) Neat PVDF, (b) Neat 70-30 PVDF-PA6 blends, (c) Blend with 3 wt. % p-MWCNT, (d) Blend with 3 wt. % PTCD-MWCNT, (e)Blend with 3 wt. % PTCD-MWCNTs+NH2 functionalized BT

Table 1: Percentage of PVDF with β-Fraction

Matrix	**β -Fraction**
Neat PVDF	0.33
Neat 70-30 PVDF-PA6 Blend	0.38
70-30 PVDF-PA6 p-MWCNT	0.37
70-30 PVDF-PA6 PTCD-MWCNT	0.36
70-30 PVDF-PA6 PTCD-MWCNT+BT-NH2	0.34

IJRAME

INTERNATIONAL JOURNAL OF RESEARCH IN AERONAUTICAL AND MECHANICAL ENGINEERING
WWW.IJRAME.COM
ISSN (ONLINE): 2321-3051

Emerging Trends in Mechanical Engineering Proceedings of the International Conference, ETME-2017, 27 & 28 December, 2017, Pg: -102-113

Effect of nanoparticle on crystallization morphology and phase preference: effect of various nanoparticles:

Figure 2 (b and a) shows the DSC exotherms for the various PVDF/PA6 blends. The crystallization temperature of neat PVDF is recorded at 139 °C. The PVDF/PA6 is a classic example of an immiscible blends that exhibit 2 distinct exotherm peak. Figure 2(a) and figure 2(b) represents the crystalline exotherms of the PVDF and PA6 matrix respectively. The binary matrix is a highly polar system, both PVDF and PA6 are highly polar materials. Due to low viscosity and interfacial energy of PA6 and MWCNT at 250 ^{0} C, it should provide good wetting process and the compartmentalization of MWCNTs in the PA6 phase. The shift in crystallization peak of PA6 further confirms the presence of MWCNTs in PA6. An observation can be made that there is no nucleating agent or in this case the nano particle that propagates the crystal formation in the PVDF phase. Interestingly, we see peak shift and a bimodal shape of the crystallization exotherm of PA6. The DSC suggests that the gamma fraction is highly dependent on the attendance of the long fibrillar MWCNTs[20]. While the thermodynamically stable α-phase are formed where the MWCNTs do not influence the folding of the tethered PA6 molecules, the gamma-phase are formed along the MWCNTs where the PA6 are wrapped around the MWCNTs and PTCD-MWCNTs and a layer by layer stacking of independent PA-6 chain could be expected. MWCNTs renders as an ideal nucleating site providing crystal growth at higher temperatures while undercooling. Only α-phase crystals are induced at higher temperatures and the crystal structure continues to grow as the temperature decreases. It is interesting to know that nanocomposites with particles other than MWCNTs (PA6/clay), the formation of the γ-phase is observed at lower temperatures[21-23]. Surprisingly, in case of the blends with PTCD-MWCNT and `BT-NH_2, PA6 resulted in single crystal structure. It could be suspected that the NH_2 functionalization on the BT nano-particle react with the PTCD group that are adsorbed on to the MWCNT to form imide bond that restrict the efficient wrapping and stacking of the PA6 chains around the MWCNTs. However, it is evident that it does not restrict the organization of the crystallites and the more thermodynamically stable α-structure is predominant. Since the crystallization temperature of PA6 here is slightly higher, it could be suggested that the NH2 functionalized BT nano-particle acts as a nucleating agent that helps form the α-phase. In this batch, it is interesting to notice that the crystallization temperature of PVDF is slightly higher than the neat PVDF. It ascribes that the BT nanoparticles also acts as nucleating sites for the PVDF phase due to the hydrogen bonding between BT-NH_2 and PVDF.

IJRAME

INTERNATIONAL JOURNAL OF RESEARCH IN AERONAUTICAL AND MECHANICAL ENGINEERING
WWW.IJRAME.COM
ISSN (ONLINE): 2321-3051

Emerging Trends in Mechanical Engineering Proceedings of the International Conference, ETME-2017, 27 & 28 December, 2017, Pg: -102-113

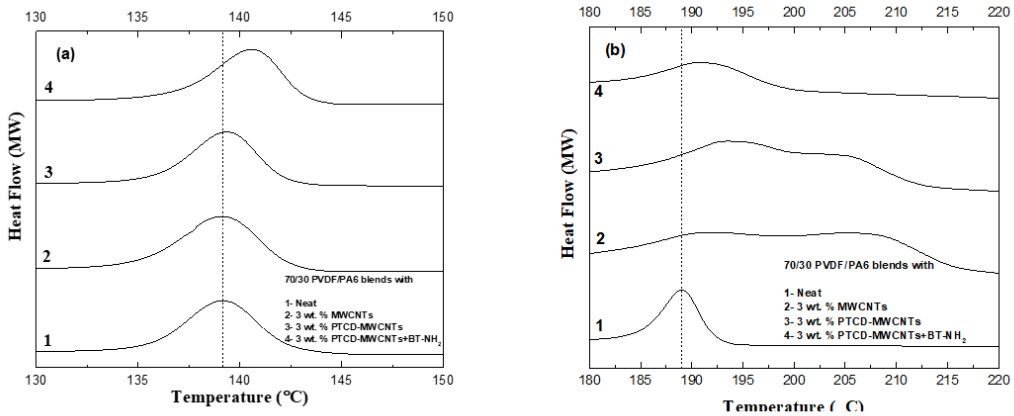

Figure: 2 DSC of (a) PVDF crystallization peak and (b) PA-6 Crystallization peak of different blend compositions

The connecting network of nanoparticles: assessing through electrical conductivity:

Figure 3. shows the AC electrical conductivity of the 70/30 blend with varying filler combination (3% wt. p-MWCNT, 3% wt. PTCD-MWCNT, 3% wt. PTCD-MWCNT+5% vol. BT-NH2). MWCNTs are excellent conductors of electricity due to the abundant electron availability along its surface. This is attributed to the stable resonance of the sp2 hybridized orbitals that have a bonding and anti-bonding orbitals which coincide at a k point, meaning, with a slight potential difference the excited electrons jump from the valence band to the conduction band, irrespective of the wavelength, making MWCNTs a semimetal. The electrical conductivity depends on factors such as size, distribution, concentration and surface treatment of the conducting additive. The aspect ratio and dispersion plays a key role in determining the percolation threshold in the matrix. Non covalent functionalization of the MWCNTs helps in attaining better dispersion by dissipating the Van der Waals' force between the nano-tubes. On the down side, a covalent functionalization might help in the dispersion of the MWCNTs but decrease the conducting nature of the material significantly as they introduce defects on the surface of the material hindering the electron flow. Coupling excellent conductivity and good geometrical contact between the nano-tube, this interconnected mesh like structure of MWCNTs actually mimics the working of the faraday's cage. It is important for the morphology of the phase that contains the conducting element, in this case MWCNTs, maintains a co-continuous morphology to have a well-connected network. In the previous section, it is established that MWCNTs are present in the PA-6 phase and it is reported that the percolating threshold of well dispersed MWCNTs is 3% wt. The net weight percentage of

IJRAME

INTERNATIONAL JOURNAL OF RESEARCH IN AERONAUTICAL AND MECHANICAL ENGINEERING
WWW.IJRAME.COM
ISSN (ONLINE): 2321-3051

Emerging Trends in Mechanical Engineering Proceedings of the International Conference, ETME-2017, 27 & 28 December, 2017, Pg: -102-113

MWCNTs in PA6 is calculated to be 10.3, considerably well above the percolating threshold. The AC conductivity for 3% MWCNT loading is of the order 10^{-7}. Further, PTCD modified 3% wt. MWCNT showed an increase in conductivity by an order of 2. The structure of PTCD is such that the sp2 bonds form a π-π stacking along the length of the MWCNTs. This facilitates the dispersion by overcoming the van der Waals between the MWCNTs which results in a better percolated structure across the PA-6 phase. It can be concluded that due to the π-π stacking between the perylene group and the MWCNT, there is an increase in electron density along the surface of the MWCNTs which results in better conductivity of the percolated nano-tubes.

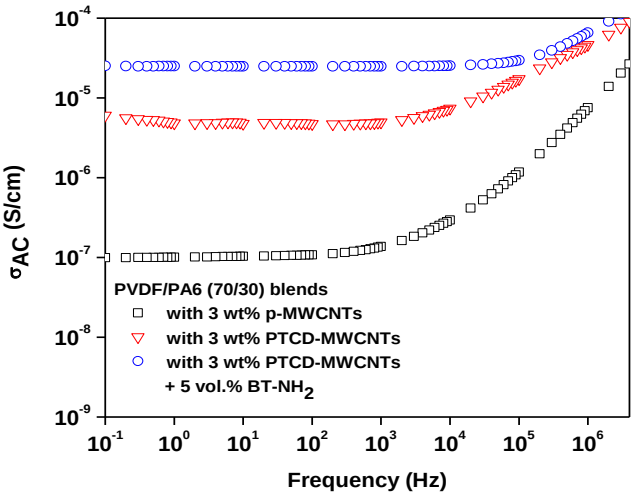

Figure 3: Room temperature AC conductivity as a function of frequency

Attenuation of EM radiation in PVDF/PA6 blends: the effect of electrically conducting (p-MWCNTs) and dielectric nanoparticles (BT-NH2):

From EM theory it is well understood that for attenuation of EM radiation material should possess electrical conductivity, however very high conductivity is not necessary. Interestingly, in case of polymer nanocomposites, attenuation can be enhanced by well-connected network of conducting fillers. The dispersion of nanoscopic fillers is great challenge. Here, we have studied effect of p-MWCNTs dispersion and its effect of attenuation properties using vector network analyzer. The SE_T is a ratio of power transmitted through specimen and incident power and can be expressed as follow.

IJRAME

INTERNATIONAL JOURNAL OF RESEARCH IN AERONAUTICAL AND MECHANICAL ENGINEERING
WWW.IJRAME.COM
ISSN (ONLINE): 2321-3051

Emerging Trends in Mechanical Engineering Proceedings of the International Conference, ETME-2017, 27 & 28 December, 2017, Pg: -102-113

$$SE_T(dB) = -20log\frac{E_T}{E_I} = -20log\frac{H_T}{H_I} = -10log\frac{P_T}{P_I}$$

The SE_T can be estimated through scattering parameters extracted from VNA using following relation.

$$SE_T(dB) = 10log\frac{1}{|S_{12}|^2} = 10log\frac{1}{|S_{21}|^2}$$

Figure 4. depicts total shielding effectiveness (SE_T) as a function of frequency in X and Ku-band for various PVDF/PA6 (70/30) blends. It is clearly evident that attenuation scales with frequency and remarkably higher SET is noted in Ku-band frequencies. The blends with 3 wt. % p-MWCNTs manifested SET of -16 dB at 18 GHz frequency. Interestingly, blends with PTCD-MWCNTs showed remarkable enhancement in X-band frequencies whereas slight enchantment was noted in ku-band frequencies. This could be attributing to enhanced dispersion of MWNTs assisted by PTCD modification which is also supported by electrical conductivity analysis. Since, the SET scales with electrical conductivity, an enhanced SET in case of blends with PTCD-MWCNTs is due to increased electrical conductivity. The blends with PTCD-MWCNT and BT-NH2 manifest no significant effect of BT-NH2 on attenuation and SET of 20 dB was noted at 18 GHz frequency. This could be due to the given concentration of BT-NH2 is not sufficient to absorb electric field associated with EM radiation and attenuation is mostly governed by PTCD-MWCNTs. In order understand mechanism behind EM attenuation we closely analyzed reflection loss (RL) values of blends with various nanoparticles.

The RL can be calculated using well established line theory from relative permittivity and permeability as shown in following relation.

$$\mathrm{RL} = 20 * \log\frac{|\mathrm{Z_{in}} - 1|}{|\mathrm{Z_{in}} + 1|}$$

Where, RL is reflection loss and normalized input incidence is denoted as Zin which can be written as follow.

$$\mathrm{Z_{in}} = \sqrt{\frac{\mu_r}{\varsigma_r}}\tanh\left[\mathrm{i}\,\frac{2\pi \mathrm{fd}}{\mathrm{c}}\sqrt{\mu_r\varsigma_r}\right]$$

IJRAME

INTERNATIONAL JOURNAL OF RESEARCH IN AERONAUTICAL AND MECHANICAL ENGINEERING
WWW.IJRAME.COM
ISSN (ONLINE): 2321-3051

Emerging Trends in Mechanical Engineering Proceedings of the International Conference, ETME-2017, 27 & 28 December, 2017, Pg: -102-113

Where, μ_r and ς_r corresponds to the relative permeability and permittivity, specimen thickness is denoted as t. The f and c are frequency and speed of light in vacuum, respectively. Figure 4 depicts RL as a function of frequency in broad band range. The minimum reflection peak in RL is corresponding to the absorption of EM radiations. Interestingly, blends with different nanoparticles manifested minimum reflection at different frequency range. In case of blends with PTCD-MWCMTs, RL of -58.6 dB was recorded at 9.3 GHz frequency. However, addition of BT-NH2 the frequency corresponding to minimum reflection was remarkably shifted to higher frequency. The band width was extended over entire X-band frequencies for all the blends. Interestingly in Ku-band frequencies, the blends with PTCD-MWCNTs and blends with PTCD-MWCMTs and BT-NH2 manifested significantly extended band width over blends with only p-MWCNTs. These observations provide clear understanding about materials which can be used for various types of application according to frequencies.

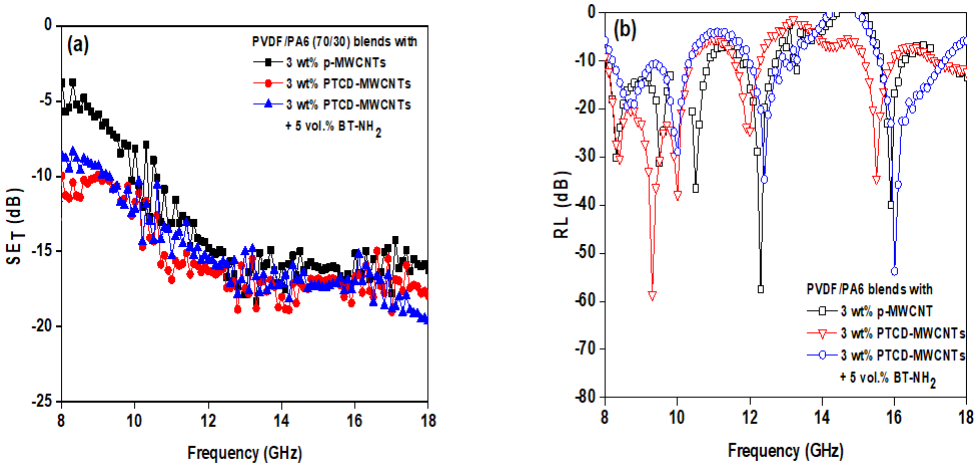

Figure 4: (a) Total shielding effectiveness as a function of frequency, (b) Reflection Loss as a function of frequency

IJRAME

INTERNATIONAL JOURNAL OF RESEARCH IN AERONAUTICAL AND MECHANICAL ENGINEERING
WWW.IJRAME.COM
ISSN (ONLINE): 2321-3051

Emerging Trends in Mechanical Engineering Proceedings of the International Conference, ETME-2017, 27 & 28 December, 2017, Pg: -102-113

Conclusion:

In summary, it can be clearly observed that the presence of conducting percolated structure in the minority co-continuous phase (PA6) can provide electromagnetic shielding in the form of reflection. Addition of non-covalent functionalization of MWCNTs with PTCD improves dispersion confirmed by electrical conductivity. It is seen that the conductivity increases from 10^{-7} S/cm to 10^{-5} S/cm which represents better overall connectivity across the morphology. The inclusion of the high K material (BT) does not hinder the interconnection network as seen in figure 3. Blends with PTCD-MWCMTs show RL of -58.6 dB at 9.3 GHz frequency. Compartmentalization of the high dielectric constant BT-NH_2 and conducting MWCNTs enhances the efficiency of the shielding property (RL) at higher frequency (16 GHz) due to the absorption of the internal reflection by the high dielectric constant material. This system can be used to shield microwave emitting appliances.

References:

1. N. Awanis Hashim, Y. Liu and K. Li, Chemical Engineering Science, 2011, 66, 1565-1575.
2. P. Martins, A. C. Lopes and S. Lanceros-Mendez, Progress in Polymer Science, 2014, 39, 683-706.
3. M. Sharma, G. Madras and S. Bose, Physical Chemistry Chemical Physics, 2014, 16, 14792-14799.
4. M. Sharma, M. P. Singh, C. Srivastava, G. Madras and S. Bose, ACS applied materials & interfaces, 2014, 6, 21151-21160.
5. M. Benz, W. B. Euler and O. J. Gregory, Macromolecules, 2002, 35, 2682-2688.
6. R. Gregorio and R. C. CapitãO, Journal of Materials Science, 2000, 35, 299-306.
7. M. Sharma, K. Sharma and S. Bose, The Journal of Physical Chemistry B, 2013, 117, 8589-8602.
8. P. Sajkiewicz, A. Wasiak and Z. Gocłowski, European polymer journal, 1999, 35, 423-429.
9. R. Gregorio, Journal of Applied Polymer Science, 2006, 100, 3272-3279.
10. R. Gregorio Jr and N. C. P. de Souza Nociti, Journal of Physics D: Applied Physics, 1995, 28, 432.
11. V. Bhingardive, M. Sharma, S. Suwas, G. Madras and S. Bose, RSC Advances, 2015, 5, 35909-35916.
12. P. Xavier and S. Bose, Rsc Advances, 2014, 4, 55341-55348.

IJRAME

INTERNATIONAL JOURNAL OF RESEARCH IN AERONAUTICAL AND MECHANICAL ENGINEERING
WWW.IJRAME.COM
ISSN (ONLINE): 2321-3051

Emerging Trends in Mechanical Engineering Proceedings of the International Conference, ETME-2017, 27 & 28 December, 2017, Pg: -102-113

13. R. Rohini and S. Bose, ACS applied materials & interfaces, 2014, 6, 11302-11310.
14. M. Sharma, S. Sharma, J. Abraham, S. Thomas, G. Madras and S. Bose, Materials Research Express, 2014, 1, 035003.
15. N. Joseph, S. K. Singh, R. K. Sirugudu, V. R. K. Murthy, S. Ananthakumar and M. T. Sebastian, Materials Research Bulletin, 2013, 48, 1681-1687.
16. S. Maiti, N. K. Shrivastava, S. Suin and B. Khatua, ACS applied materials & interfaces, 2013, 5, 4712-4724.
17. J. Zhu, S. Wei, N. Haldolaarachchige, D. P. Young and Z. Guo, The Journal of Physical Chemistry C, 2011, 115, 15304-15310.
18. G. Arlt and D. Hennings, Journal of applied physics, 1985, 58, 1619-1625.
19. C. Muralidhar and P. Pillai, Journal of materials science letters, 1987, 6, 1243-1245.
20. I.Y. Phang, J. Ma, L. Shen, T. Liu and W. D. Zhang, Polymer International, 2006, 55, 71-79.
21. A.-C. Brosse, S. Tencé-Girault, P. M. Piccione and L. Leibler, Polymer, 2008, 49, 4680-4686.
22. T. Liu, W. C. Tjiu, C. He, S. S. Na and T.-S. Chung, Polymer International, 2004, 53, 392-399.
23. Z. Zhao, W. Zheng, W. Yu, H. Tian and H. Li, Macromolecular Rapid Communications, 2004, 25, 1340-1344.